

# Transitional Grid Maps: Efficient Analytical Inference of Dynamic Environments under Limited Sensing

José Manuel Gaspar Sánchez<sup>1</sup>, Leonard Bruns<sup>2</sup>, Jana Tumova<sup>2</sup>, Patric Jensfelt<sup>2</sup> and Martin Törngren<sup>1</sup>

**Abstract**—Autonomous agents rely on sensor data to construct representations of their environment, essential for predicting future events and planning their own actions. However, sensor measurements suffer from limited range, occlusions, and sensor noise. These challenges become more evident in dynamic environments, where efficiently inferring the state of the environment based on sensor readings from different times is still an open problem. This work focuses on inferring the state of the dynamic part of the environment, i.e., where dynamic objects might be, based on previous observations and constraints on their dynamics. We formalize the problem and introduce Transitional Grid Maps (TGMs), an efficient analytical solution. TGMs are based on a set of novel assumptions that hold in many practical scenarios. They significantly reduce the complexity of the problem, enabling continuous prediction and updating of the entire dynamic map based on the known static map (see Fig. 1), differentiating them from other alternatives. We compare our approach with a state-of-the-art particle filter, obtaining more prudent predictions in occluded scenarios and on-par results on unoccluded tracking.

## I. INTRODUCTION

The representation of the environment used by autonomous agents generally includes two components: the static and the dynamic part. The static part is often used for localization and global path planning and can be pre-computed or generated as the autonomous system explores. In contrast, the dynamic part of the environment, i.e., the set of dynamic obstacles, is typically used for local planning since the ego agent needs to react to it.

A classical approach to represent the dynamic obstacles of the environment is to keep a list of known obstacles and track them independently, known as multi-target tracking [1]. The main challenge of this approach is the data association problem, i.e., knowing if a new measurement corresponds to an existing track or not. Grid-based approaches are an alternative to multi-target tracking which do not suffer from the data association problem since they do not represent individual obstacles with tracks; they represent the environment as a set of cells. When the environment can be assumed static, each cell can be modeled individually and new measurements can be incorporated using Bayes' formula, as in [2]–[4]. When the environment cannot be assumed static, the

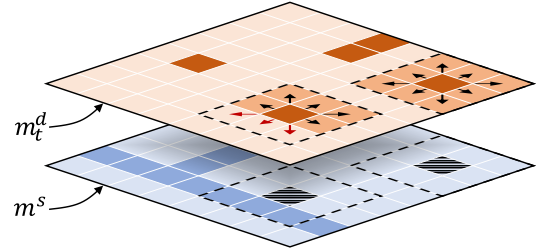


Fig. 1. Transitional Grid Map (TGM). The dynamic environment at the current time,  $m_t^d$ , is predicted based on the transition probability between cells, represented with arrows, and the known static environment,  $m^s$ , which limits invalid transitions.

temporal and spatial relations between cells can be modeled as a Bayesian network, as in [5], [6]. Unfortunately, in the general case, probabilistic inference in Bayesian networks is NP-hard [7], which makes some of the approaches developed in this area computationally intractable unless they introduce significant simplifications, such as only updating the portion of the map in the current field of view of the agent.

Instead, our approach performs the prediction and update over the entire map. The main idea is to maintain information about areas from where dynamic obstacles could emerge, including previously seen areas that are temporally out of the field of view and areas that have never been seen.

### A. Contributions

This work studies *the inference of the dynamic part of the environment with limited sensing assuming knowledge about the static environment*. The main contributions are:

- 1) a mathematical formulation of the problem of inferring the dynamic part of the environment, analyzing where the computation becomes intractable;
- 2) formulating assumptions that hold in many practical scenarios and allow for the problem to be simplified, i.e., to obtain an analytical solution that can be computed in real-time; and
- 3) a method with a simple and efficient implementation that achieves better results in occluded scenarios and on-par results on unoccluded tracking compared to state-of-the-art approaches.

### B. Related Work

Traditional occupancy grid maps (OGMs), [2]–[4], are used to fuse multiple sensor measurements into a unified representation of the environment. The environment is modeled as a set of cells, each of which has a binary state, occupied or free. Assuming a static environment and independence

\*This research has been carried out as part of the TECoSA Vinnova Competence Center for Trustworthy Edge Computing Systems and Applications.

<sup>1</sup>José Manuel Gaspar Sánchez and Martin Törngren are with the Mechanics Division, KTH Royal Institute of Technology, 100 44 Stockholm, Sweden (email: jmgs@kth.se; martint@kth.se).

<sup>2</sup>Leonard Bruns, Jana Tumova and Patric Jensfelt are with the Division of Robotics, Perception and Learning, KTH Royal Institute of Technology, 100 44 Stockholm, Sweden (email: leonardb@kth.se; tumova@kth.se; patric@kth.se).

between the cells, the probability of occupancy of each cell of the map can be computed individually.

However, the real world is often not static. When this assumption is not met, the original formulation of the traditional grid map method trusts previous beliefs over new contradicting measurements; it takes the same number of observations to change the state of a cell as past observations that were used to set it [8].

The method proposed in [9] uses a hidden Markov model (HMM) for each cell to represent both the belief about the state of the cell and the corresponding probability of state change. While this approach explicitly models how occupancy changes over time, each cell is represented individually, which ignores that obstacles cannot suddenly appear but must have traveled to it from another neighboring cell. Also employing an HMM, [10] additionally incorporates observations from neighboring cells at the previous time step when estimating the state of each cell. However, when no observations in neighboring cells are available, e.g., during occlusions, their model only relies on the individual cell state. We instead assume a transition model between cells, which makes cells dependent on the belief about the previous state of neighboring cells, regardless of whether they are occluded or not.

Other authors have used particle filters to represent dynamic obstacles [11]–[13]. Most of them make use of the Dempster-Shafer theory of evidence [14], [15], which allows to only populate cells with particles where there is some evidence of occupancy. This approach, used to reduce computation, implies that areas outside the current field of view due to occlusions or limited sensor range are not populated with particles.

A different particle filter, derived using random finite sets (RFS), is proposed in [16]. The authors' initial approach represents potential obstacles in unobserved areas with particles. However, many scenarios have large unobserved areas, which renders the approach computationally intractable [16]. To address this, the authors also apply the Dempster-Shafer theory of evidence, reducing the computation to recently observed areas, similarly to other particle filters. In contrast, our method allows us to efficiently update the entire map, including areas previously seen that are temporally out of the field of view and areas that have never been seen before and are populated with a prior.

A pure Bayesian particle filter, without the Dempster-Shafer theory, is presented in [17] to keep track of occluded areas. This filter also populates particles in occluded areas to represent the hypotheses of possible unseen obstacles, leading to a drastic increase in the number of particles generated. Computation times are not analyzed in this work, but because of the number of particles required, it may not be suitable for a real-time implementation.

More recently, learning-based methods operating on grids have been proposed to perceive and predict dynamic obstacles [18], [19]. These approaches, while showing promising results, still require extensive training and their performance depends on the quality of the available data.

### C. Problem Formulation

We consider an agent with known poses up to the current time  $t$ ,  $x_{1:t} = \{x_1, x_2, \dots, x_t\}$ , equipped with a sensor similar to a 2D laser scanner. The sensor has a limited range, is limited by occlusions and is subject to noise. It produces a set of measurements  $z_{1:t} = \{z_1, z_2, \dots, z_t\}$ . The agent moves in a semi-dynamic environment, i.e., populated by dynamic and static obstacles. The static obstacles are known beforehand through a map. The problem at hand is to estimate the dynamic part of the environment.

## II. METHOD

To address this problem, we model the environment at each time  $t$ ,  $m_t$ , as a set of  $N$  cells, i.e.,  $m_t = \{m_{t,1}, m_{t,2}, \dots, m_{t,N}\}$ . Each cell can be in one of three possible states: free, static (occupied by a static obstacle), or dynamic (occupied by a dynamic obstacle); i.e.,  $m_{t,i} \in \{f, s, d\}$ . We also define the binary variables  $m_{t,i}^s = \llbracket m_{t,i} = s \rrbracket$  and  $m_{t,i}^d = \llbracket m_{t,i} = d \rrbracket$ , where  $\llbracket \cdot \rrbracket$  denotes Iverson brackets. For simplicity of the notation, the variable denoting if a cell is static,  $m_i^s$ , will be referred to without the time index since they are assumed to not change over time. The static part of the environment,  $m^s = \{m_1^s, m_2^s, \dots, m_N^s\}$ , is assumed to not change over time. In contrast, dynamic obstacles are able to move through space, meaning that the state of a dynamic cell can transition to nearby cells over time, with the restriction that they can never move to a static cell.

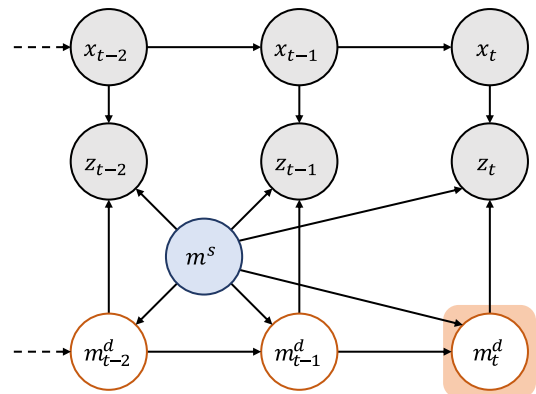


Fig. 2. Bayesian network of the problem of inferring the state of the dynamic part of an environment. Poses  $x_{1:t}$ , measurements  $z_{1:t}$ , and the static part of the environment  $m^s$  are known, and the goal is to estimate  $m_t^d$ , the current state of the dynamic part of the environment.

Given our proposed modeling, the problem becomes to estimate the current state of the dynamic part of the environment,  $m_t^d = \{m_{t,1}^d, m_{t,2}^d, \dots, m_{t,N}^d\}$ , given that we know the static part of the environment,  $m^s$ , the poses,  $x_{1:t}$ , and measurements,  $z_{1:t}$ , up to the current time. The probabilistic graphical model of the problem is shown in Figure 2.

Starting at the same assumption as the original grid mapping algorithm for static environments, we assume that the problem can be broken down into the estimation of individual cells, such that the posterior of the map is approximated as

the product of its marginals [2]–[4]:

$$p(m_t^d | z_{1:t}, x_{1:t}, m^s) \approx \prod_i p(m_{t,i}^d | z_{1:t}, x_{1:t}, m^s). \quad (1)$$

Following the derivations in (2)–(7), with the changes **highlighted**, the odds can be computed as

$$\frac{p(m_{t,i}^d | z_{1:t}, x_{1:t}, m^s)}{p(-m_{t,i}^d | z_{1:t}, x_{1:t}, m^s)} = \underbrace{\frac{p(m_{t,i}^d | z_t, x_t, m^s)}{1 - p(m_{t,i}^d | z_t, x_t, m^s)}}_{\text{current observations}} \underbrace{\frac{p(m_{t,i}^d | z_{1:t-1}, x_{1:t-1}, m^s)}{1 - p(m_{t,i}^d | z_{1:t-1}, x_{1:t-1}, m^s)}}_{\text{prediction}} \underbrace{\frac{1 - p(m_{t,i}^d | m^s)}{p(m_{t,i}^d | m^s)}}_{\text{prior}}. \quad (8)$$

The first and third terms of the expression in (8) are trivial to compute. The first one (“current observations”) refers to the probability of a cell being dynamic given only the current sensor readings, the pose and the known static map  $p(m_{t,i}^d | z_t, x_t, m^s)$ . This term can be easily computed with an appropriate inverse sensor model, with the only difference being that known static cells should be ignored when populating the dynamic map. The third one (“prior”), refers to the prior assigned to the cell at the current time step only knowing the static map,  $p(m_{t,i}^d | m^s)$ .

The second term (“prediction”) contains all the complexity. It reflects the probability of a cell being currently dynamic given all the previous sensor readings and poses of the agent, and the static map  $p(m_{t,i}^d | z_{1:t-1}, x_{1:t-1}, m^s)$ . Even if there existed an accurate prediction model,  $p(m_{t,i}^d | m_{t-1}^d, m^s)$ , the dynamic environment at the previous time step,  $m_{t-1}^d$ , is still uncertain, as it can only be estimated based on the agent’s previous locations and sensor readings,  $p(m_{t-1}^d | z_{1:t-1}, x_{1:t-1}, m^s)$ . The computation of this term involves marginalizing over all the possible dynamic maps at the previous time step (13), which grows exponentially with the size of the map and becomes unfeasible to compute. Section II-A introduces the main assumptions under which this term can be simplified. Section II-B describes how, under those assumptions, we obtain an analytical solution.

### A. Random Transitions

$T_{j,i}$  denotes the event that the content of cell  $j$  transitions to cell  $i$  between two consecutive time steps. Based on  $T_{j,i}$ , the state of a cell after a transition can be defined as

$$p(m_{t,i}^d | T_{j,i}, m^s, m_{t-1}^d) = m_{t-1,j}^d, \quad (9)$$

$$p(m_{t,i}^s | T_{j,i}, m^s, m_{t-1}^d) = m_{t-1,j}^s, \quad (10)$$

i.e., if the event  $T_{j,i}$  occurs, the content of cell  $j$  at time  $t-1$  deterministically moves into cell  $i$  at time  $t$ . To prevent dynamic obstacles from being able to move to a static cell (see Fig. 1), the probability of transition is assumed to depend on the static map,  $m^s$ , as follows:

$$p(T_{j,i} | m^s) = \begin{cases} D_{j,i} \overline{m_i^s} \overline{m_j^s}, & \text{if } j \neq i \\ m_i^s + \overline{m_i^s} (D_{i,i} + \sum_{k \neq i} [D_{i,k} m_k^s]), & \text{if } j = i \end{cases} \quad (11)$$

The initial distribution,  $D$ , can be seen as the probability of a transition between two cells if there were no static cells around. In the presence of static cells, the transition probability  $p(T_{j,i})$  is modified in (11) as follows:

- 1) The probability of a transition between two different cells is equal to 0 if any of the two cells are static.
- 2) The probability of staying in the same cell,  $p(T_{i,i})$ , becomes 1 if the cell is static.
- 3) The probability of staying in the same cell,  $p(T_{i,i})$ , is also increased according to the number of other transitions that are not possible due to static cells in the neighborhood, making a dynamic obstacle surrounded by static cells more likely to stay in the same position.

The prediction model  $p(m_{t,i}^d | m_{t-1}^d, m^s)$  can now be obtained by marginalizing over all possible  $T_{j,i}$ :

$$\begin{aligned} p(m_{t,i}^d | m_{t-1}^d, m^s) &= \sum_j [m_{t-1,j}^d p(T_{j,i} | m^s, m_{t-1}^d)] \\ &= m_{t-1,i}^d p(T_{i,i} | m^s, m_{t-1}^d) + \sum_{j \neq i} [m_{t-1,j}^d p(T_{j,i} | m^s, m_{t-1}^d)] \\ &= m_{t-1,i}^d \left( D_{i,i} + \sum_{k \neq i} [D_{i,k} m_k^s] \right) + \overline{m_i^s} \sum_{j \neq i} [m_{t-1,j}^d D_{j,i}]. \end{aligned} \quad (12)$$

---


$$p(m_{t,i}^d | z_{1:t}, x_{1:t}, m^s) = \frac{p(z_t | m_{t,i}^d, z_{1:t-1}, x_{1:t}, m^s) p(m_{t,i}^d | z_{1:t-1}, x_{1:t}, m^s)}{p(z_t | z_{1:t-1}, x_{1:t}, m^s)} \quad \text{Bayes rule} \quad (2)$$

$$= \frac{p(z_t | m_{t,i}^d, z_{1:t-1}, x_{1:t}, m^s) p(m_{t,i}^d | z_{1:t-1}, x_{1:t-1}, m^s)}{p(z_t | z_{1:t-1}, x_{1:t}, m^s)} \quad \text{Independence} \quad (3)$$

$$\approx \frac{p(z_t | m_{t,i}^d, x_t, m^s) p(m_{t,i}^d | z_{1:t-1}, x_{1:t-1}, m^s)}{p(z_t | z_{1:t-1}, x_{1:t}, m^s)} \quad \text{Markov assumption*} \quad (4)$$

$$= \frac{p(m_{t,i}^d | z_t, x_t, m^s) p(z_t | x_t, m^s) p(m_{t,i}^d | z_{1:t-1}, x_{1:t-1}, m^s)}{p(m_{t,i}^d | x_t, m^s) p(z_t | z_{1:t-1}, x_{1:t}, m^s)} \quad \text{Bayes rule} \quad (5)$$

$$= \frac{p(m_{t,i}^d | z_t, x_t, m^s) p(z_t | x_t, m^s) p(m_{t,i}^d | z_{1:t-1}, x_{1:t-1}, m^s)}{p(m_{t,i}^d | m^s) p(z_t | z_{1:t-1}, x_{1:t}, m^s)} \quad \text{Independence} \quad (6)$$

$$\frac{p(m_{t,i}^d | z_{1:t}, x_{1:t}, m^s)}{p(-m_{t,i}^d | z_{1:t}, x_{1:t}, m^s)} = \frac{p(m_{t,i}^d | z_t, x_t, m^s)}{1 - p(m_{t,i}^d | z_t, x_t, m^s)} \frac{p(m_{t,i}^d | z_{1:t-1}, x_{1:t-1}, m^s)}{1 - p(m_{t,i}^d | z_{1:t-1}, x_{1:t-1}, m^s)} \frac{1 - p(m_{t,i}^d | m^s)}{p(m_{t,i}^d | m^s)} \quad \text{Odds} \quad (7)$$

## B. The Resulting Prediction Model

When including the random transition model from (12), the probability of a cell being occupied given the previous poses and measurements can be simplified as shown in (13)-(17). It is important to highlight that this prediction model does not require marginalizing over all the  $2^N$  possible dynamic maps at the previous time-step,  $m_{t-1}^d$ , making the computation feasible.

## C. Transition Probability Independent of Absolute Location

So far, for simplicity of the notation, cells have been referenced by one index, e.g.,  $i$  or  $j$ . In this section, they are referenced by their  $x$  and  $y$  components. In some cases, the initial probability of transition between two cells does not depend on the absolute position of those cells, but only on the relative position between them, such that  $D[\Delta x, \Delta y] = D[x_i - x_j, y_i - y_j] = D_{j,i}$ . In those cases, the prediction can be simplified as a set of operations involving a couple of 2D convolutions of the static and dynamic maps.

We define  $M^s$  and  $M^d$  as functions storing the known static map and the previously estimated dynamic map:

$$M^s[x_i, y_i] = m_i^s, \quad (18)$$

$$M^d[x_i, y_i] = p(m_{t-1,i}^d | z_{1:t-1}, x_{1:t-1}). \quad (19)$$

We also define the kernel  $K$  as the initial probability of transition for different cells, and  $K'$ , its flipped version:

$$K[\Delta x, \Delta y] = D[\Delta x, \Delta y] \mathbb{I}[\Delta x, \Delta y \neq 0], \quad (20)$$

$$K'[\Delta x, \Delta y] = D[-\Delta x, -\Delta y] \mathbb{I}[\Delta x, \Delta y \neq 0]. \quad (21)$$

In this case, the prediction term from (17) can be simplified to the following expression, involving a pair of discrete 2D convolutions, denoted by  $**$ :

$$\frac{p(m_{t,i}^d | z_{1:t}, x_{1:t}, m^s)}{p(m_{t,i}^d | z_{1:t}, x_{1:t}, m^s)} = \underbrace{\frac{1 - p(m_{t,i}^d | m^s)}{p(m_{t,i}^d | m^s)}}_{\text{prior}} \underbrace{\frac{p(m_{t,i}^d | z_t, x_t, m^s)}{1 - p(m_{t,i}^d | z_t, x_t, m^s)}}_{\text{current observations}}$$

$$\frac{M^d[x_i, y_i](D_0 + (M^s ** K')[x_i, y_i]) + (1 - M^s[x_i, y_i])(M^d ** K)[x_i, y_i]}{\underbrace{M^d[x_i, y_i](D_0 + (M^s ** K')[x_i, y_i]) + (1 - M^s[x_i, y_i])(M^d ** K)[x_i, y_i]}_{\text{prediction}}}, \quad (22)$$

where  $D_0$  denotes  $D[0, 0]$ .

With this model, the filter works by sequentially smoothing out the previous belief according to where dynamic obstacles can move within the static map and, subsequently, integrating the new observations into the smoothed out belief.

## D. Decay Factor

Depending on the application, it might be relevant to prevent the method from becoming overconfident about sparsely populated areas that were observed a long time ago. This is achieved by averaging the prediction term in log odds with the prior log odds based on a decay factor  $\delta$ :  $(1 - \delta) \text{logit}(p(m_{t,i} | m^s)) + \delta \text{logit}(p(m_{t,i}^d | z_{1:t-1}, x_{1:t-1}, m^s))$ . This ensures that the cells tend towards the prior when they are not observed. Lastly, after reverting to odds and combining with the previous prior from (22):

$$\frac{p(m_{t,i}^d | z_{1:t}, x_{1:t}, m^s)}{p(m_{t,i}^d | z_{1:t}, x_{1:t}, m^s)} = \underbrace{\left[ \frac{1 - p(m_{t,i}^d | m^s)}{p(m_{t,i}^d | m^s)} \right]^\delta}_{\text{prior}} \underbrace{\frac{p(m_{t,i}^d | z_t, x_t, m^s)}{1 - p(m_{t,i}^d | z_t, x_t, m^s)}}_{\text{current observations}}$$

$$\frac{\underbrace{M^d[x_i, y_i](D_0 + (M^s ** K')[x_i, y_i]) + (1 - M^s[x_i, y_i])(M^d ** K)[x_i, y_i]}_{\text{prediction}}}{\underbrace{M^d[x_i, y_i](D_0 + (M^s ** K')[x_i, y_i]) + (1 - M^s[x_i, y_i])(M^d ** K)[x_i, y_i]}_{\text{prediction}}}. \quad (23)$$

## E. Transition Model

The previous subsections of the method assume that the initial distribution of the random transitions between cells,  $p(D_{j,i})$ , is known. This distribution could be learned, similarly to [20] or [10], or it could be derived from a model. In this work, the latter approach has been chosen, since learning a model requires application-specific data.

We assume a maximum speed at which an obstacle can move,  $v_{\max}$ , which, together with the time step  $\Delta t$ , limits the distance  $d_{\max} = v_{\max} / \Delta t$  that the content of a cell can move in one time step. In our experiments, we assume a uniform distribution, i.e., it is equally likely that the content of a cell moves to any of the cells within the distance  $d_{\max}$ :

$$D[x, y] = \begin{cases} 1/n & \sqrt{x^2 + y^2} \leq d_{\max} \\ 0 & \text{otherwise,} \end{cases} \quad (24)$$

where  $n$  is the number of inputs,  $[x, y]$ , that satisfy the condition,  $\sqrt{x^2 + y^2} \leq d_{\max}$ .

$$p(m_{t,i}^d | z_{1:t-1}, x_{1:t-1}, m^s) = \sum_{m_{t-1}^d} \left[ p(m_{t,i}^d | m_{t-1}^d, m^s) p(m_{t-1}^d | z_{1:t-1}, x_{1:t-1}, m^s) \right] \quad (13)$$

$$= \sum_{m_{t-1}^d} \left[ \left( p(m_{t-1,i}^d | m_{t-1}^d) \left( D_{i,i} + \sum_{j \neq i} [D_{i,j} m_j^s] \right) + \overline{m_i^s} \sum_{j \neq i} \left[ p(m_{t-1,j}^d | m_{t-1}^d) D_{j,i} \right] \right) p(m_{t-1}^d | z_{1:t-1}, x_{1:t-1}, m^s) \right] \quad (14)$$

$$= \left( D_{i,i} + \sum_{j \neq i} [D_{i,j} m_j^s] \right) \sum_{m_{t-1}^d} \left[ p(m_{t-1,i}^d | m_{t-1}^d) p(m_{t-1}^d | z_{1:t-1}, x_{1:t-1}, m^s) \right] + \overline{m_i^s} \sum_{m_{t-1}^d} \sum_{j \neq i} \left[ p(m_{t-1,j}^d | m_{t-1}^d) D_{j,i} p(m_{t-1}^d | z_{1:t-1}, x_{1:t-1}, m^s) \right] \quad (15)$$

$$= \left( D_{i,i} + \sum_{j \neq i} [D_{i,j} m_j^s] \right) p(m_{t-1,i}^d | z_{1:t-1}, x_{1:t-1}, m^s) + \overline{m_i^s} \sum_{j \neq i} \left[ D_{j,i} \sum_{m_{t-1}^d} \left[ p(m_{t-1,j}^d | m_{t-1}^d) p(m_{t-1}^d | z_{1:t-1}, x_{1:t-1}, m^s) \right] \right] \quad (16)$$

$$= \left( D_{i,i} + \sum_{j \neq i} [D_{i,j} m_j^s] \right) p(m_{t-1,i}^d | z_{1:t-1}, x_{1:t-1}, m^s) + \overline{m_i^s} \sum_{j \neq i} \left[ D_{j,i} p(m_{t-1,j}^d | z_{1:t-1}, x_{1:t-1}, m^s) \right] \quad (17)$$

### III. EXPERIMENTS

We study the behavior of the proposed method in three different experiments. In Section III-A, we show a qualitative comparison between our proposed method (TGM), an occupancy grid map (OGM), and the recent particle filter-based approach (RFS) by Nuss et al. [16] on an environment with static and dynamic elements. In Section III-B, we present a quantitative evaluation between TGM and RFS. Finally, in Section III-C, we show an implementation of our method running on an embedded system using ROS. Our proposed method was implemented using (23). For the OGM and RFS, the existing implementations from MATLAB have been used.

#### A. Qualitative Evaluation

We first consider the scenario depicted in the first column of Figure 3. The static environment includes a corridor at the top connected to rooms 1 and 2, and room 3 which is connected to room 2. The ego agent is tasked to move from the left side of the corridor to the right side and back, without getting into any collision with the static environment, the dynamic obstacle traversing the corridor in the opposite direction, or any possibly occluded dynamic obstacle. The predicted occupancy (current for the OGM) within the next 2 seconds has been used with the A\* algorithm to plan a collision-free trajectory ( $P_{occ} \leq P_{th}$ ).

Initially, the ego agent can detect the corridor and room 1, while rooms 2 and 3 are completely unobserved. At that point, the standard grid map (Fig. 3.d) can be used to obtain a path to the goal, but this does not take into account the possible obstacles that could enter the corridor from room 2. In the case of the RFS approach (Fig. 3.g), the method predicts that something could appear from the wall splitting rooms 1 and 2 since the method does not take a map of

the static environment as input. More importantly, similarly to the standard grid map, it is unable to predict something entering the corridor from room 2. This is due to the particles not being populated in occluded areas, as mentioned in [16]. Our proposed method (Fig. 3.j) correctly predicts that the cells close to the occlusion could become occupied.

At  $t=26$ , the ego agent can observe that room 2 is also empty while room 1 gets out of sight. The standard grid map (Fig. 3.e) remembers room 1 free since unobserved cells are not updated. In contrast, in the RFS approach (Fig. 3.h), the occupancy of room 1 decays based on how long the cells have been unobserved. In the case of the TGM (Fig. 3.k), since room 1 is not reachable by any obstacle (observed or occluded), the probability of occupancy in the room stays close to 0. It is important to highlight that this behavior is not hard-coded, but emerges from the transition model and the knowledge about the static environment.

Once the agent has reached the end of the corridor, it is tasked to return back. In the OGM (Fig. 3.f), both rooms 1 and 2 are remembered as empty. In the case of the RFS approach (Fig. 3.i), the probability of occupancy in both rooms has increased due to the time the cells have been unobserved, but they are not predicted to be able to reach the corridor due to the lack of particles in occluded areas. In our proposed approach (Fig. 3.l), room 1 is still unoccupied, and room 2 is predicted to have possible occupancy coming from room 3, but it does not reach far enough to make the agent deviate from a straight path.

Both TGM and the RFS have parameters that control how quickly the confidence about temporarily unobserved areas decay;  $\delta$  and  $\alpha$  respectively. However, due to the lack of particle updates in occluded areas, there is no value of  $\alpha$  that allows RFS to achieve the same result as our proposed TGM,

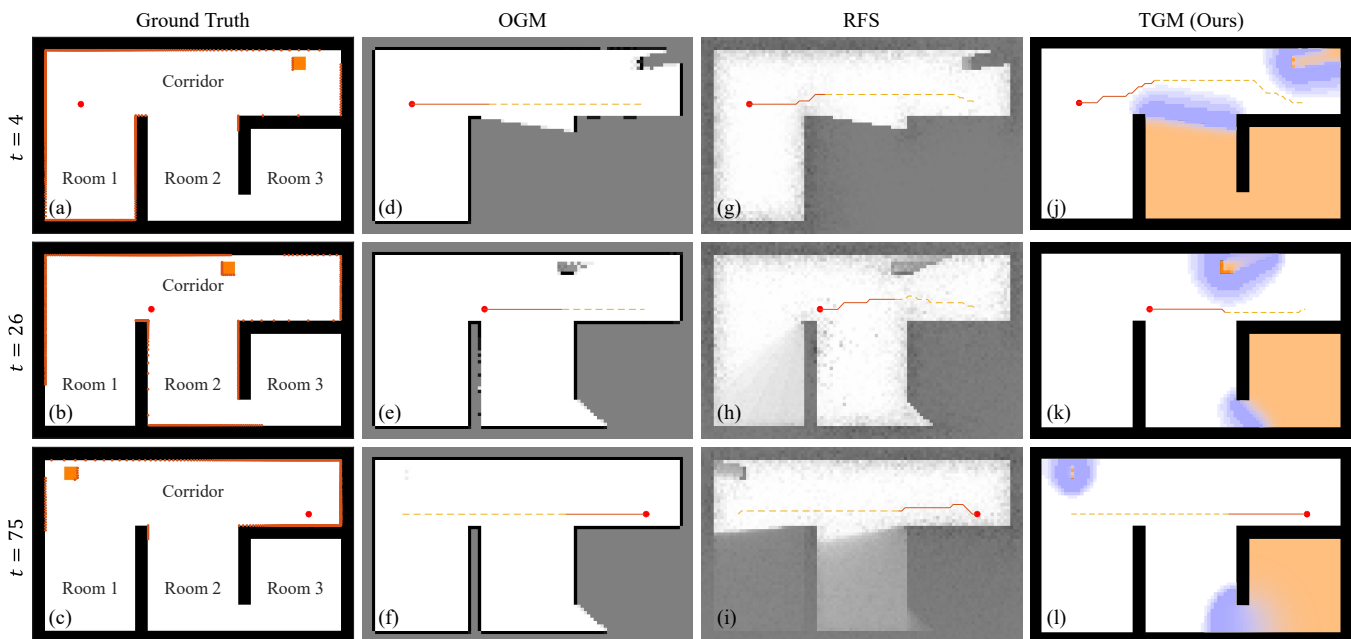


Fig. 3. (a)-(c) Ground truth scenario. The ego agent is shown as a red dot, the static environment in black and the dynamic obstacle in orange. (d)-(f) Occupancy probability for the occupancy grid map. (g)-(i) Predicted occupancy probability for the RFS. (j)-(l) Current probability of occupancy (in orange) and cells where the predicted occupancy probability is bigger than the threshold (in purple) for the TGM.

i.e., that room 1 is remembered empty while also realizing that some dynamic obstacle could reach room 2.

### B. Quantitative Evaluation of Fully Dynamic Environment

We now compare the RFS and TGM methods. We exclude the OGMs since they are not optimized for obstacle tracking. We run 100 randomized scenarios, with different parameters, for a total of 1400 simulations. To ensure a fair comparison, none of the scenarios has static elements. The ego agent is placed at the center of the scenario while dynamic obstacles move around it. The number of dynamic obstacles is randomly selected between 1 and 5, with their positions initialized within the field of view of the ego agent. Initial velocities of dynamic obstacles are randomly set between 0 and  $v_{\max}=0.5\text{m/s}$ . The simulated dynamic obstacles collide elastically with each other and bounce back if they are about to leave the ego agent’s field of view. An example scenario is illustrated in Figure 4.

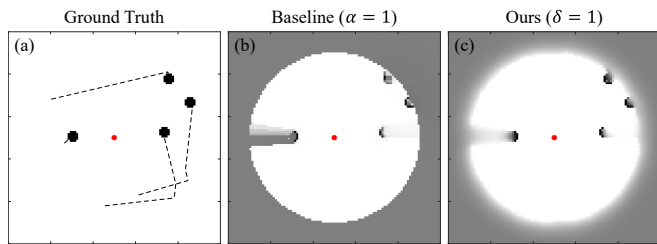


Fig. 4. (a) Ground truth scenario. (b) Occupancy probability for RFS with  $\alpha=1$ . (c) Occupancy probability for TGM with  $\delta=1$ .

For each randomly generated scenario, both methods were run with different parameters. We varied  $\alpha$  and  $\delta$  in the range of 0.7 to 1 for the baseline and our method, respectively.

Figure 5.a shows for each parameter the average error, i.e., the mean difference between the ground truth state of each cell and the inferred probability of occupancy. The mean error of our proposed method is lower across all parameter

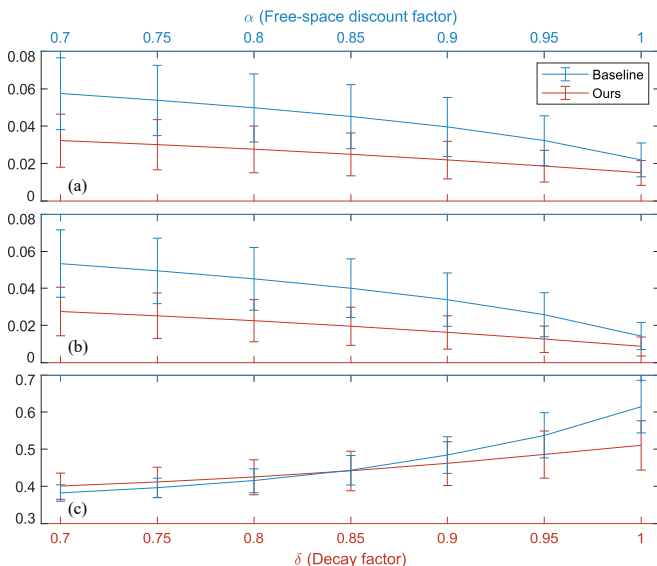


Fig. 5. (a) Average error in the probability of occupancy. (b) Average error for free cells. (c) Average error for occupied cells.

settings and the difference becomes smaller as  $\alpha$  and  $\beta$  get closer to 1. Both of them decrease as the methods are set less conservatively, i.e., higher values of  $\alpha$  and  $\delta$ . Figure 5.b shows the average error for free cells. The results are similar to Figure 5.a since most cells of the scenarios are free.

Figure 5.c shows the average error for occupied cells. The error increases as the methods are set less conservatively, showing again the trade-off between not being over-conservative about areas that have recently fallen outside the field of view and accurately predicting which cells could be occupied. The baseline achieves minimally better results for small values of  $\alpha$  at the cost of larger error in free space.

These simulations have been performed using an Intel i7-12700H processor. The baseline required  $71\pm 3.6\text{ms/cycle}$  compared to the  $7.2\pm 0.7\text{ms/cycle}$  by our proposed method. While these results are only representative of this set of random scenarios, they indicate a significant reduction in computation time, in line with the simplicity of Eq. (23).

### C. Real-World Implementation

In the last experiment, we demonstrate that our method can be efficiently run on an embedded device. The method has been implemented as a ROS node and executes locally on the Raspberry Pi 3 of a TurtleBot3 with an average of  $30.2\pm 5.5\text{ms/cycle}$ . The TurtleBot in the back keeps track of a person in a room while it also predicts that more dynamic obstacles could appear from an unobserved area (Figure 6).

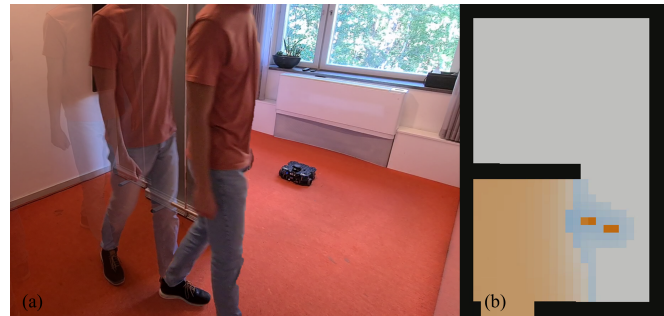


Fig. 6. (a) Example scenario for the real-world implementation. (b) RViz visualization of the map produced by the ROS node. The known static map is shown in black, the dynamic map is shown in orange, and the predicted occupancy is shown in blue. RViz was run on a remote computer.

## IV. CONCLUSIONS AND FUTURE WORK

This work formalizes the problem of inferring the state of the dynamic part of the environment and introduces Transitional Grid Maps (TGMs) as an analytical solution. TGMs are built upon a set of novel assumptions that significantly reduce the complexity of the problem, enabling continuous prediction and updating of the entire map, distinguishing them from other alternatives.

The method could be extended to include velocity estimates by expanding the 2D grid representation of the environment to a 4D grid, similarly to [6], which would increase the computational requirements. Additionally, classification information obtained from other sensors, such as cameras, could be incorporated into the grid, allowing for different transition models per class.

## REFERENCES

- [1] C.-C. Wang, C. Thorpe, S. Thrun, M. Hebert, and H. Durrant-Whyte, "Simultaneous localization, mapping and moving object tracking," *The International Journal of Robotics Research*, vol. 26, no. 9, pp. 889–916, 2007.
- [2] A. Elfes, "Using occupancy grids for mobile robot perception and navigation," *Computer*, vol. 22, no. 6, pp. 46–57, 1989.
- [3] H. Moravec and A. Elfes, "High resolution maps from wide angle sonar," in *Proceedings of the IEEE International Conference on Robotics and Automation*, vol. 2, 1985, pp. 116–121.
- [4] H. P. Moravec, "Sensor fusion in certainty grids for mobile robots," in *Sensor Devices and Systems for Robotics*. Springer, 1989, pp. 253–276.
- [5] C. Coue, T. Fraichard, P. Bessiere, and E. Mazer, "Using Bayesian programming for multi-sensor multi-target tracking in automotive applications," in *Proceedings of the IEEE International Conference on Robotics and Automation*, vol. 2, 2003, pp. 2104–2109.
- [6] C. Coué, C. Pradalier, C. Laugier, T. Fraichard, and P. Bessière, "Bayesian occupancy filtering for multitarget tracking: An automotive application," *The International Journal of Robotics Research*, vol. 25, no. 1, pp. 19–30, 2006.
- [7] G. F. Cooper, "The computational complexity of probabilistic inference using bayesian belief networks," *Artificial Intelligence*, vol. 42, no. 2-3, pp. 393–405, 1990.
- [8] M. Yguel, O. Aycard, and C. Laugier, "Update policy of dense maps: Efficient algorithms and sparse representation," in *Field and Service Robotics*. Springer, 2008, pp. 23–33.
- [9] D. Meyer-Delius, M. Beinhofer, and W. Burgard, "Occupancy grid models for robot mapping in changing environments," in *Proceedings of the AAAI Conference on Artificial Intelligence*, vol. 26, no. 1, 2012, pp. 2024–2030.
- [10] Z. Wang, R. Ambrus, P. Jensfelt, and J. Folkesson, "Modeling motion patterns of dynamic objects by IOHMM," in *Proceedings of the IEEE/RSJ International Conference on Intelligent Robots and Systems*, 2014, pp. 1832–1838.
- [11] S. Steyer, G. Tanzmeister, and D. Wollherr, "Object tracking based on evidential dynamic occupancy grids in urban environments," in *IEEE Intelligent Vehicles Symposium (IV)*, 2017, pp. 1064–1070.
- [12] —, "Grid-based environment estimation using evidential mapping and particle tracking," *IEEE Transactions on Intelligent Vehicles*, vol. 3, no. 3, pp. 384–396, 2018.
- [13] G. Tanzmeister and D. Wollherr, "Evidential grid-based tracking and mapping," *IEEE Transactions on Intelligent Transportation Systems*, vol. 18, no. 6, pp. 1454–1467, 2017.
- [14] A. P. Dempster, "A generalization of Bayesian inference," *Journal of the Royal Statistical Society. Series B (Methodological)*, vol. 30, no. 2, pp. 205–247, 1968.
- [15] G. Shafer, *A Mathematical Theory of Evidence*. Princeton University Press, 1976.
- [16] D. Nuss, S. Reuter, M. Thom, T. Yuan, G. Krehl, M. Maile, A. Gern, and K. Dietmayer, "A random finite set approach for dynamic occupancy grid maps with real-time application," *The International Journal of Robotics Research*, vol. 37, no. 8, pp. 841–866, 2018.
- [17] N. Rexin, D. Nuss, S. Reuter, and K. Dietmayer, "Modeling occluded areas in dynamic grid maps," in *Proceedings of the IEEE International Conference on Information Fusion (FUSION)*, Jul. 2017, pp. 1–6.
- [18] J. Dequaire, P. Ondrůška, D. Rao, D. Wang, and I. Posner, "Deep tracking in the wild: End-to-end tracking using recurrent neural networks," *The International Journal of Robotics Research*, vol. 37, no. 4-5, pp. 492–512, Apr. 2018. [Online]. Available: <http://journals.sagepub.com/doi/10.1177/0278364917710543>
- [19] M. Schreiber, V. Belagiannis, C. Gläser, and K. Dietmayer, "Dynamic Occupancy Grid Mapping with Recurrent Neural Networks," in *2021 IEEE International Conference on Robotics and Automation (ICRA)*, May 2021, pp. 6717–6724.
- [20] T. Kucner, J. Saarinen, M. Magnusson, and A. J. Lilienthal, "Conditional transition maps: Learning motion patterns in dynamic environments," in *Proceedings of the IEEE/RSJ International Conference on Intelligent Robots and Systems*, 2013, pp. 1196–1201.